AIAA 80-1701R

Voyager 1 Saturn Targeting Strategy

Robert J. Cesarone*
Jet Propulsion Laboratory, California Institute of Technology, Pasadena, Calif.

The trajectory targeting strategy for the Voyager 1 Saturn encounter was designed to accommodate predicted uncertainties in Titan's ephemeris while maximizing spacecraft safety and science return. The encounter was characterized by a close Titan flyby 18 h prior to Saturn periapse. Retargeting of the nominal trajectory to account for late updates in Titan's estimated position can disperse the ascending node location, which is nominally situated at a radius of low expected particle density in Saturn's ring plane. The strategy utilized a floating Titan impact vector magnitude to minimize this dispersion. Encounter trajectory characteristics and an actual targeting history are presented.

Introduction

THE complex flyby geometry and precision science objectives of the Voyager 1 Saturn encounter required a complex and novel targeting strategy for this spacecraft. Some previous interplanetary flyby missions relied on less complex targeting strategies which fixed the aimpoint in the target body's B-space well in advance of the actual encounter. Other missions employed adaptive strategies tailored to their own requirements and different from those of Voyager 1.

Two factors led to the complexity of the Voyager 1 Saturn targeting strategy. These were the rapid flybys of two massive bodies, Titan and Saturn, within 18 h and the key targeting events which dictated severe geometric constraints. The specific targeting events were 1) a diametric (across the diameter) or maximum duration occultation of Earth by Titan, 2) a fixed time of exit from Earth occultation by Saturn, and 3) passage through the ring plane at a fixed distance from Saturn. The first two objectives support radio occultation experiments, whereas the last is a safety feature, allowing Saturn ring plane crossing in a region thought to be swept clean by the satellite Dione (Dione clear zone). The changing estimates of the Titan ephemeris altered the flyby geometry of the encounter trajectory and resulted in dispersions in the above events. These dispersions are called targeting errors to differentiate them from the more familiar delivery errors (orbit determination uncertainties and maneuver execution errors), which were the dominant errors in some previous interplanetary flyby missions. A targeting strategy which fixes the B-space aimpoint too early is not able to reduce or eliminate targeting errors and so is not sufficient to guarantee adequate achievement of science and safety requirements. A floating Titan impact vector strategy which can reduce or eliminate these errors was developed for Voyager 1 and is presented here. Gray and Van Allen[1] have also examined the role of targeting errors in the Voyager 1 Jupiter flyby, in which rapid encounters with Jupiter and Io and the desire to penetrate the Io flux tube created analogous types of targeting challenges.

First some background information is provided on previous mission targeting strategies, the nominal Saturn encounter trajectory, the Saturn ring system, and the Titan ephemeris uncertainties. Then the effect of retargeting the trajectory to take Titan position updates into account is examined. Strategies which fix the spacecraft aimpoint in the Titan B-plane are shown to lead to targeting errors. The floating Titan impact vector strategy is then developed. Additional implications of this strategy are presented and a targeting history of the actual encounter is described.

Early Targeting Strategies

Three previous interplanetary flyby missions which provide insight into targeting strategies prior to Voyager are the Mariner Mars 1969 dual-spacecraft (Mariners 6 and 7) mission, the Mariner Venus-Mercury (Mariner 10) 1973 mission, and the Pioneer 10 and 11 missions to Jupiter and Saturn. Although a number of other missions have been flown, these were chosen as a representative sample.

Mariners 6 and 7 were launched in February and March 1969 with Mars encounters in July and August of that year.[2] Each trajectory was corrected by one midcourse maneuver in March and April 1969, respectively. Thus the final design aimpoints were selected shortly (within days) after launch and four to five months before the Mars encounters. This is an example of fixed B-space targeting, since the aimpoints were selected early and not updated based on increased orbital knowledge. Fixed targeting worked very well since the science aim zones were not severely constrained and no flybys of massive bodies, other than Mars itself, occurred to disperse the trajectories.

The Mariner 10 mission was more adaptive, having to contend with severe spacecraft anomalies and the desire to include nominal flybys of Venus and Mercury plus two additional extended mission Mercury encounters, while being propellant constrained.[3,4] The roll gyro anomaly which occurred shortly before the Venus encounter resulted in the need to place restrictions on allowable spacecraft attitudes. This and the application of "second" body targeting (i.e., pre-Venus to Mercury 1, etc.) made the mission very demanding. In addition the Mercury 1 flyby was characterized by a critical "free-return" aim zone requirement. Finally, the Mercury 2 and 3 aimpoints were only chosen well after Mercury 1 and were subject to updates based on continuing science and mission analysis and spacecraft status estimates. The Mariner 10 mission employed targeting strategies which were complex but different from that of Voyager 1 at Saturn. Specifically, no massive bodies other than the target planets themselves had to be considered in the Mariner 10 targeting.

The Pioneer 10 and 11 missions flew the first spacecraft to encounter Jupiter in 1973 and 1974. Pioneer 11 also continued on to encounter Saturn in 1979.[5,6] In addition to satisfying Jupiter science requirements, the Pioneer 10 spacecraft was targeted for an occultation of Earth by Io.[7] Hence it was necessary to accommodate the motion and position uncertainty of Io. This required precise arrival time control, although some tolerance on the aimpoint spatial components was allowed. The Pioneer 10 flyby was somewhat analogous to the Voyager 1 flybys of Jupiter/Io and Titan/Saturn.

Presented as Paper 80-1701 at the AIAA/AAS Astrodynamics Conference, Danvers, Mass., Aug. 11-13, 1980; submitted Sept. 16, 1980; revision received July 13, 1981. This paper is declared a work of the U.S. Government and therefore is in the public domain.

*Engineer, Mission Design Section. Member AIAA.

Table 1 Voyager 1 Saturn encounter trajectory events

Event	Date	Time (GMT)	Time from Saturn CA, h	Distance, km
Titan CA	11/12/80	05:40:41	−18.09	6969
Enter Titan-sun occultation		05:46:22	−17.99	
Enter Titan-Earth occultation		05:47:33	−17.97	
Exit Titan-sun occultation		05:57:06	−17.81	
Descending node		05:58:09	−17.79	1,184,575
Exit Titan-Earth occultation		05:59:45	−17.77	
Tethys CA		22:15:52	− 1.50	415,855
Saturn CA[a]		23:45:50	0	184,497
Closest Mimas in light	11/13/80	00:37:41	+0.86	108,432
Mimas CA[b]		01:42:32	+1.95	88,996
Enter Saturn-Earth occultation		01:43:16	+1.96	
Enceladus CA		01:50:36	+2.08	202,796
Enter Saturn-sun occultation		01:56:54	+2.18	
Exit Saturn-sun occultation		02:37:24	+2.86	
Exit Saturn-Earth occultation		03:10:35	+3.41	
Enter ring-Earth occultation		03:19:40	+3.56	
Closest Dione in light		03:28:13	+3.71	161,543
Exit ring-Earth occultation		03:35:09	+3.82	
Dione CA[c]		03:39:00	+3.89	161,285
Ascending node		04:20:06	+4.57	377,902
Rhea CA		06:21:13	+6.59	72,797
Hyperion CA		16:44:01	+16.97	879,277

CA = closest approach. [a] One-way light time = 1 hr, 24 min, 47 s. [b] Mimas is in darkness at CA. [c] Dione is in darkness at CA.

However, Pioneer 10 position updates for Io were determined exclusively from Earth-based observations and thus the final Jupiter targeting awaited only the processing of these data. The Voyager 1 Jupiter and Saturn targeting, however, had to await processing of optical images of Io and Titan which were taken only days before the encounters. This fact and the need to control all three aimpoint components necessitated the added flexibility in the Voyager targeting.

The targeting of Pioneer 11 at Jupiter was somewhat more complex than that of its sister ship. Until Pioneer 10 Jupiter science objectives were achieved, alternate Pioneer 11 target options were maintained. After the successful flyby of the first spacecraft, the Pioneer 11 Jupiter B-plane aimpoint was fixed by the decision to continue on to Saturn.[8] However the choice of arrival time, to achieve the desired flyby orientation with the magnetic field, was left open, pending the development of the field model from the recent Pioneer 10 data. This demanded additional targeting flexibility for Pioneer 11 at Jupiter.

The final Pioneer 11 Saturn targeting was done after the Jupiter flyby. Two aimpoint options were retained until early 1979, when the decision was made to target outside the rings. This aimpoint was selected in order to duplicate and verify the relative safety of the planned Voyager 2 Saturn ring plane crossing. After this decision, the nominal Pioneer 11 Saturn B-space aimpoint was fixed.

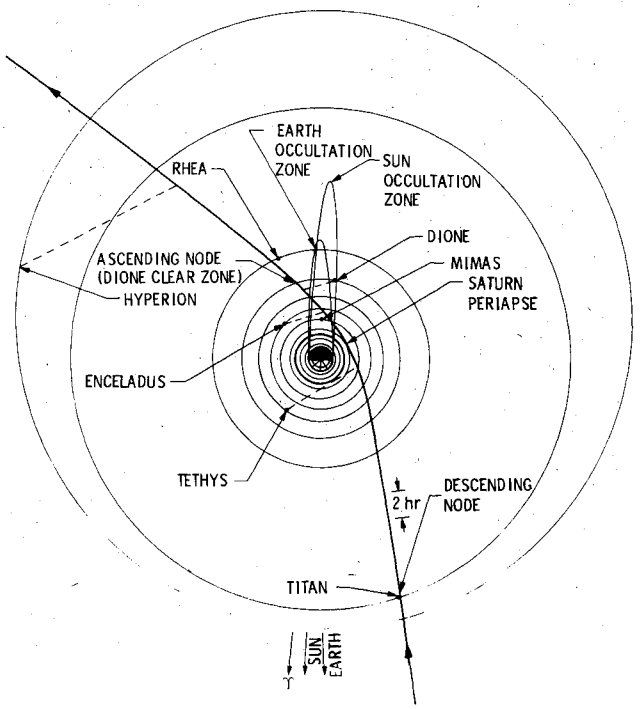

Fig. 1 Saturn equatorial plane view of Voyager 1 encounter trajectory.

Encounter Trajectory Characteristics

Voyager 1 encountered the planet Saturn on Nov. 12, 1980, at a nominal spacecraft event time of 23:45:50 GMT. The closest approach (CA) was 184,500 km or 3.1 radii from the planet center, which corresponds to 125,000 km from the Saturnian cloud tops. Other significant trajectory events occurred before and after Saturn periapse. Table 1 lists these events in chronological order. Figure 1 shows a Saturn equatorial plane projection of the encounter trajectory.

About 18 h prior to Saturn periapse, Voyager 1 encountered the satellite Titan (at about 4000 km altitude), the only moon in the solar system known to have an appreciable atmosphere. Determination of the temperature of Titan's cloud tops and estimation of surface temperature and pressure were among the highest priority objectives of the Voyager 1 encounter. Measurements made by Pioneer 11 in September 1979 indicated Titan cloud top temperatures of 80 ± 10 K.[9] To allow determination of Titan atmospheric parameters, Voyager 1 performed a radio occultation experiment, which occurred just minutes after the Titan closest approach, when the spacecraft disappeared behind Titan as seen from Earth. This critical mission event, which lasted only 12 min, is pictured in Fig. 2.

As shown in the figure, this occultation is diametric, a geometry which is highly desirable for the design of the radio occultation experiment. This will be discussed in detail later. In addition, Voyager 1 also achieved a 12 min solar oc-

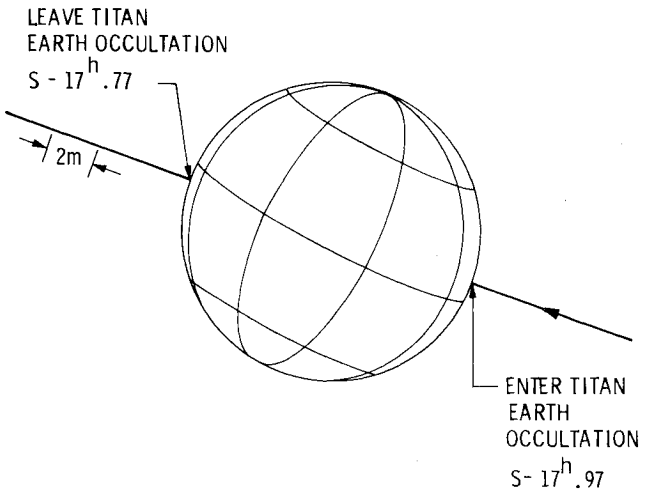

Fig. 2 Earth view of Titan during Earth occultation.

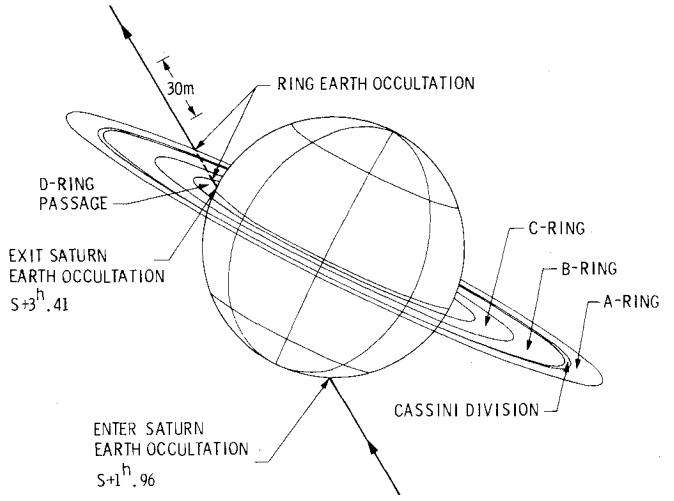

Fig. 3 Earth view of Saturn system during Saturn-Earth occultation and ring-Earth occultation.

cultation by Titan. During the Earth occultation by Titan, the spacecraft traversed the first of its two node crossings with the Saturn ring plane. This descending node occurred at just under 20 Saturn radii (Saturn radius $\simeq$60,000 km), where ring material is not a concern.

About 16 h after the descending node, the spacecraft encountered the satellite Tethys. This was a distant flyby ($\sim$416,000 km) as Tethys was on the opposite side of Saturn at this time. An hour and a half later the spacecraft made its closest approach to Saturn itself. At this time Voyager 1 was 117,500 km below the ring plane. The planet subtended an angle of almost 38 deg as seen from the spacecraft or more than 10 times the linear dimensions of the field of view of the Voyager wide-angle camera.

After Saturn periapse, trajectory events occurred rapidly. The closest approach with Mimas, at a range of 89,000 km, occurred while the satellite was in the shadow of Saturn. The smallest range to Mimas while it was lighted was 108,000 km. Next the Earth and sun occultations by Saturn occurred. Figure 3 shows the Saturn-Earth occultation, which lasted about 90 min, and the ring-Earth occultation. Figure 3 also shows the nearly equatorial exit from the Saturn-Earth occultation.[10] This exit geometry and its timing were very important to the radio science occultation experiment and were two of the main drivers for the targeting strategy to be employed. The Enceladus closest approach ($\sim$203,000 km) occurred during the Saturn-Earth occultation. Dione was encountered during the ring occultation at a range of about 161,500 km. However, it was in the shadow of Saturn at this time. About 11 min later, Dione was lighted and at nearly the same distance.

Finally, the trajectory ascending node was reached, about 4.5 h after the Saturn closest approach. This node necessarily occurred around 6.3 Saturn radii. Earth-based observations have indicated the presence of ring material at this distance.[11] This is the Saturn E-ring, whose existence may have presented a hazard to Voyager 1. Thus, to maximize spacecraft safety, the nominal trajectory was designed with an ascending node placed within the Dione clear zone. This is a region of the E-ring which is thought to have been swept clear of particles by the satellite Dione. The desire to constrain the trajectory ascending node to this zone was an additional driver for the targeting strategy.

The Rhea closest approach ($\sim$73,000 km) occurred 2 h after the ascending node. This close encounter presented challenges to the Voyager imaging activities since trajectory knowledge uncertainties used to plan these activities were greatly magnified by the Titan and Saturn flybys. This also impacted the targeting strategy and will be discussed later. The Hyperion closest approach ($\sim$879,000 km), the last significant event planned for the Saturn flyby, occurred 10 h after Rhea.

Saturn E-Ring and Clear Zones

The planet Saturn is characterized by three main visible rings. These include the C-ring at 1.20-1.53 radii from the planet center, the B-ring at 1.53-1.96 radii, and the A-ring at 2.01-2.28 radii. The Cassini Division lies between the B- and A-rings. There is a D-ring within the C-ring and finally the F-ring outside the A-ring, as discovered by Pioneer 11.[12] However, the Saturn E-ring was most important to Voyager 1. Although the Pioneer 11 spacecraft was not able to detect this ring visually, recent Earth-based observations[13] during the edge-on ring alignment and the Pioneer 11 micrometeoroid detector results[14] have confirmed its existence. The E-ring is thought to extend outward from the visible rings to about 8 Saturn radii or possibly beyond. In contrast to the visible rings, it is also considered that this ring may have a substantial thickness.

Since this proposed E-ring model includes the orbits of Mimas through Rhea, it is felt that these satellites would sweep out ring material in a region about their mean orbits. These regions of reduced density are known as clear zones. Due to science considerations at Titan and Saturn,[10] the Voyager 1 trajectory ascending node was necessarily in the vicinity of the Dione clear zone. This zone is theoretically at 6.3 Saturn radii or 377,900 km[15] from the center of Saturn, with a width of 5520 km and a thickness of 4160 km.† The track of the spacecraft through this zone is shown in Fig. 4. Note that the angle between the Voyager 1 trajectory and the Saturn ring plane (26 deg) made it impossible to pass cleanly through the Dione clear zone. Some ring material is intercepted at the clear zone "edges." Nevertheless, a centralized Dione clear zone pass still minimizes ring particle impact probability and hence is desirable for maximizing spacecraft safety. For these reasons the Voyager 1 nominal Saturn encounter trajectory was targeted so as to pass through the center of the Dione clear zone.

Titan Ephemeris Uncertainties and Targeting Error

To maximize the safety of the Voyager 1 spacecraft, it was not enough to target the nominal encounter trajectory to the

†The actual thickness of the E-ring is an uncertain quantity. Estimates range from a few to several thousand kilometers, with a probable thickness not in excess of 2000 km. The 4160 km value, which was used for all calculations in this report, is based on the region which is (or would be) dynamically swept out by Dione. If this thickness is actually too great, a conservative analysis will result.

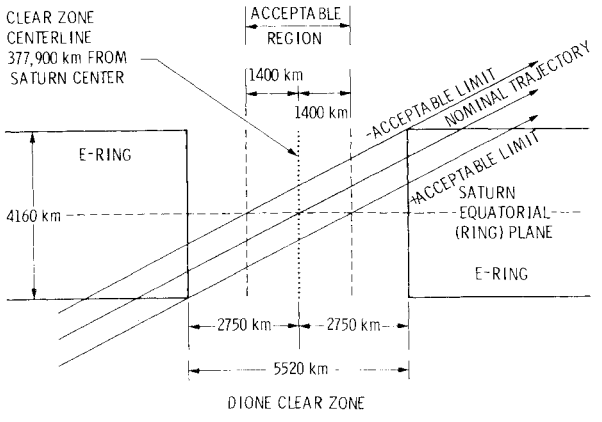

Fig. 4 Voyager 1 flight path through Dione clear zone.

Titan aimpoint which results in passage through the center of the Dione clear zone. Retargeting of the trajectory to account for late Titan ephemeris updates can cause substantial changes in the radial distance of the ascending node. As a result, a retargeted trajectory may have its ascending node altered enough so as to result in a low probability of Dione clear zone passage.

The position of Titan (and the other Saturnian satellites) relative to the planet, prior to the encounter, was obtained from Earth-based observations. These were of course subject to certain errors, which include radial uncertainties, latitude or cross-track uncertainties, and longitude or along-track uncertainties. The radial position was best determined with an uncertainty of ± 800 km 2σ ($\sim 95\%$ confidence). The latitudinal and longitudinal positions each had an uncertainty of ± 1200 km 2σ.[16] The 95% values were chosen as an acceptable level of protection for the analysis of Dione clear zone passage. A full three-dimensional covariance analysis of these Titan ephemeris errors demonstrated that the radial, latitude, and longitude uncertainties are only very slightly correlated. Thus a diagonal covariance matrix was used for the analysis.

As the spacecraft approached Saturn its cameras imaged the satellites to provide navigation information. This optical navigation system was able to reduce ephemeris uncertainties and update the position of Titan (and other satellites). This new position required retargeting of the trajectory, which could be done in a number of ways. However, certain strategies had disadvantages because they did not have the ability to accurately control the ascending node location or the timing of trajectory events. Since the node location was a safety consideration and the event timing was severely constrained by the necessities of advance sequence design, some new scheme had to be employed to take advantage of this new Titan position knowledge.

The nominal encounter trajectory was targeted so as to fly by Titan at an altitude of about 4000 km. The impact vector $\boldsymbol{B}_T$ in the Titan impact plane had a magnitude $|\boldsymbol{B}_T|$ of 7000 km. A typical targeting strategy would maintain $|\boldsymbol{B}_T| = 7000$ km in the presence of the Titan ephemeris uncertainties noted above. This requires that the trajectory be movable (relative to Saturn) by the same amount as the 95% Titan position uncertainties. However, when the trajectory is moved to follow Titan around in this manner, a dispersive effect on the radial distance of the ascending node results. This is shown in Table 2. Adjusting for a Titan radial shift has a small effect on the ascending node location. Similarly, a latitude shift results in a more substantial effect, but adjusting for a longitude shift is seen to cause the dominant effect where a 1200 km Titan longitude shift results in a radial dispersion at the ascending node of 3600 km. Table 2 also shows how many half-widths of the Dione clear zone the ascending node dispersions are equivalent to. Thus, a full 95% Titan longitude dispersion results in a complete miss of the Dione clear zone by a factor of 1.3. The probability of a clear zone passage was not very good with this type of targeting strategy.

Table 2 Dispersive effect of 95% Titan ephemeris uncertainties on ascending node location

	Titan position change		
	Radial 800 km	Latitude 1200 km	Longitude 1200 km
ΔR node, km	537	2040	3600
Dione clear zone half-widths	0.19	0.74	1.30
Required change in Titan TCA to null ΔR node, s	37	140	218

The above ascending node dispersions can be eliminated by changing the Titan arrival time for each case, thus bringing the node back into the center of the Dione clear zone. However, the time changes required to accomplish this can be substantial, especially for the Titan longitude error, as seen on the bottom line of Table 2. Since timing of science observations must be determined long before optical navigation updates the Titan ephemeris, shifting the event times by the amounts shown in Table 2 was not allowable.

These shifts in ascending node location or event timing are examples of targeting error. This type of error may be defined as a forced change in the desired encounter targeting due to a late update in some estimated parameter. The Voyager 1 Saturn encounter was subject to this type of error because the relationship between the prime mission requirements at different bodies (Titan and Saturn) was altered by late updates in the Titan ephemeris estimates. In certain cases, targeting error may be eliminated or reduced by incorporating the relevant parameter updates and a proper targeting strategy into the design of the final trajectory correction maneuvers (TCM). The penalties to be paid in this type of approach are an increase in targeting complexity and a slight degradation in science return caused by the necessity of freeing other parameters which ideally would be fixed. Delivery error, as it is used in this analysis, differs from targeting error in that it is a combination of residual trajectory uncertainty and final TCM execution errors, which cannot be corrected beyond a certain level.

Analysis indicated that there was a feasible targeting strategy which accommodated the Titan ephemeris uncertainties and reduced targeting errors. This method involved floating the magnitude of the Titan impact vector $|\boldsymbol{B}_T|$ as an additional control variable. Floating $|\boldsymbol{B}_T|$ controls the ascending node location while creating much smaller timing variations for science observations. This strategy is described in detail below. However, to see how this strategy satisfied the mission objectives, it is first necessary to identify and consider a number of the mission requirements that applied to Voyager 1 at Saturn.

Mission Requirements for Saturn Encounter

Three stringent mission requirements constrained the Voyager 1 flyby of Saturn. These were adopted to provide maximum science return while minimizing the hazard to the spacecraft.

First, the occultation of the Earth by Titan must be diametric. Radio science typically takes advantage of occultations to obtain information about a body's atmosphere, i.e., its pressure profile. This is done by means of a limb-tracking experiment in which the spacecraft antenna is moved so as to follow the image of the Earth around the limb of the occulting body. Analysis of the signal received at the Earth yields the desired atmospheric data. For the special case of a diametric occultation the virtual image of the Earth is more nearly stationary at a particular point on the occulting body's

Table 3 Event time and pointing uncertainties

Error type	Event	95% uncertainty
Delivery	Titan geocentric occultation entry[a]	30 s
Delivery	Titan geocentric occultation exit[a]	30 s
Delivery	Saturn geocentric occultation entry[a]	43 s
Delivery	Saturn geocentric occultation exit[a]	47 s
Knowledge	Rhea pointing[b]	3 mrad

[a]Based on orbit determination data to S−8.5 days (delivery epoch).
[b]Based on orbit determination data to S−18 h (knowledge epoch).

limb. Thus the radio antenna beamwidth can provide data for a wide range of atmospheric pressures. This is more realizable than a two-dimensional (off-diametric) limb-tracking experiment requiring excessively high spacecraft turn rates to follow the limb. Furthermore, the a priori knowledge of the position of Titan's limb was too poor to provide a reasonably good chance of successful limb-tracking. Thus, to maximize the probability of success of the Titan radio science experiment, a diametric occultation of the Earth was selected as a mission requirement.

Second, since it is very difficult to incorporate event time updates into previously designed sequences, it is usual to fix one trajectory event in time. For typical flyby missions periapse might be fixed for simplicity. However, periapse is not a particularly significant event from a science point of view. Since the Voyager 1 Saturn trajectory was highly constrained by science objectives, it was decided to fix a science event in time. This event was chosen to be the exit from the occultation of Earth by Saturn. The spacecraft performed a radio science experiment when in this Earth occultation zone, similar to the Titan-Earth occultation experiment except that the full two-dimensional limb-tracking maneuver was employed. Since this was a more complex operation, it was felt that success could best be enhanced by fixing the occultation exit in time. Fixing the exit also allowed good tracking performance during the important ring occultation which followed.

Third, the passage of the ascending node through the Dione clear zone was a mission requirement. This was a safety feature required since much valuable science data acquisition remained to be performed (and also later transmittal of some data previously recorded) after the ring plane crossing.

The above three requirements completely specify the three degrees of freedom available for correction by a trajectory correction maneuver (TCM). In addition to these, three other items were identified as being important for science experiments. First was the requirement for acceptable levels of statistical errors. Once the trajectory has been adjusted to accommodate the Titan ephemeris updates, there still remain statistical errors caused by the flybys of Titan and Saturn with their dispersing effect on the downstream trajectory. These include timing errors for trajectory events and pointing errors for satellite observations, particularly Rhea. These errors are shown in Table 3 for a nominal Titan $|\boldsymbol{B}_T| = 7000$ km. Initial interest in increasing the nominal $|\boldsymbol{B}_T|$ to lessen these errors subsided because the negative impact on fields and particles measurements at Titan would be severe and because the errors shown were considered acceptable.

Next, the elevation of the 64 m Deep Space Station (DSS) 63 in Spain had to be acceptably high at the time of the exit from the occultation of Earth by Saturn. This was to insure success of the limb-tracking experiment as described above. A 10 deg elevation angle was considered to be the minimum acceptable. The 7000 km nominal Titan $|\boldsymbol{B}_T|$ yielded an elevation angle of 15.3 deg.

Finally, it was desired to have the exit from the occultation of Earth occur at or near the Saturn equator. Radio science investigation of the Saturnian atmosphere is best accomplished by having the trajectory exit from behind the Saturn limb into a region that is unobscured by ring material as seen from Earth. Since the Saturn D-ring material was expected to extend close to the planet (possibly as far as the cloud tops) the best way to accomplish this desired exit was to have it occur at the Saturn equator. This exit latitude could not be strictly controlled without a much more complex targeting strategy. Instead, it was monitored for the range of trajectories to be expected with the implemented strategy. The exit latitudes were not exactly on the equator but were within a few degrees of it, which was considered acceptable.

Targeting Strategy

The three degrees of freedom of a TCM are typically stated in terms of increments of speed ($\Delta\dot{x}$, $\Delta\dot{y}$, $\Delta\dot{z}$) in the three Cartesian directions of a convenient coordinate system, usually the Earth mean equator and equinox of 1950 (EME50). However, for this strategy more insight is obtained by choosing the Titan B-plane parameters as representative of those degrees of freedom. Since there is a well-defined mapping from the Cartesian velocity increments to the Titan B-plane this poses no problem. Thus the control variables are chosen as: $|\boldsymbol{B}_T|$, the magnitude of the Titan impact vector; θ_T, the angle this vector makes with the ecliptic plane; and TF_T, the time of arrival at Titan. These new control variables are related to the three stringent mission requirements described above. To first order θ_T controls the diametricity of the Earth occultation by Titan. Also to first order TF_T controls the time of exit from the occultation of Earth by Saturn. This leaves $|\boldsymbol{B}_T|$ to control the Dione clear zone passage. In reality the Earth occultation exit time and the Dione clear zone passage are somewhat coupled and hence so are TF_T and $|\boldsymbol{B}_T|$. The important effect is the sensitivity of the ascending node radial distance to $|\boldsymbol{B}_T|$. A 1000 km change in the Titan B-plane magnitude produces about 6000 km of shift in the radial distance of the ascending node. Thus B-plane magnitude is a powerful control for Dione clear zone passage.

To accomplish the actual targeting, a 3×3 matrix of partial derivatives or sensitivities is used to relate the mission requirements or target variables back to the Titan B-plane or control variables. Thus

$$\begin{bmatrix} \Delta d_{\mathrm{OCC}_T} \\ \Delta T_{\mathrm{OCC}_S} \\ \Delta R_{C/Z} \end{bmatrix} = D \begin{bmatrix} \Delta\theta_T \\ \Delta TF_T \\ \Delta B_T \end{bmatrix} \tag{1}$$

or for retargeting

$$\begin{bmatrix} \Delta\theta_T \\ \Delta TF_T \\ \Delta B_T \end{bmatrix} = D^{-1} \begin{bmatrix} \Delta d_{\mathrm{OCC}_T} \\ \Delta T_{\mathrm{OCC}_S} \\ \Delta R_{C/Z} \end{bmatrix} \tag{2}$$

where $\Delta d_{\mathrm{OCC}_T}$ = required change in Titan-Earth occultation diametricity, km; $\Delta T_{\mathrm{OCC}_S}$ = required change in time of Saturn-Earth occultation exit, $\Delta R_{C/Z}$ = required change (in Saturn ring plane) in ascending node location, km; $\Delta\theta_T$ = required change in Titan B-vector direction, deg; ΔTF_T = required change in Titan arrival time; s ΔB_T = required change in Titan B-vector magnitude, km.

The sensitivity matrix, D is given by

$$D = \begin{bmatrix} \frac{\partial d_{OCC_T}}{\partial \theta_T} & \frac{\partial d_{OCC_T}}{\partial TF_T} & \frac{\partial d_{OCC_T}}{\partial B_T} \\ \frac{\partial T_{OCC_S}}{\partial \theta_T} & \frac{\partial T_{OCC_S}}{\partial TF_T} & \frac{\partial T_{OCC_S}}{\partial B_T} \\ \frac{\partial R_{C/Z}}{\partial \theta_T} & \frac{\partial R_{C/Z}}{\partial TF_T} & \frac{\partial R_{C/Z}}{\partial B_T} \end{bmatrix}$$

$$= \begin{bmatrix} -100.1 & -0.01443 & -0.002280 \\ -3.804 & +1.436 & +0.1625 \\ -241.0 & +14.33 & +6.1200 \end{bmatrix}$$

where numerical values for these sensitivities were obtained by independently perturbing each of the Titan B-plane parameters from those specified on a predetermined nominal trajectory. The matrix D was found to be well-conditioned and no singularity problems were encountered. Its inverse was easily obtainable and acceptably accurate.

An initial estimate of the error in the target variables can be obtained by examining the following assumed linear relationship

$$\begin{bmatrix} \Delta d_{OCC_T} \\ \Delta T_{OCC_S} \\ \Delta R_{C/Z} \end{bmatrix} = P \begin{bmatrix} \Delta \mathrm{RAD}_T \\ \Delta \mathrm{LAT}_T \\ \Delta \mathrm{LON}_T \end{bmatrix} \quad (3)$$

where $\Delta \mathrm{RAD}_T$ = Titan ephemeris shift, radial direction, km; $\Delta \mathrm{LAT}_T$ = Titan ephemeris shift, latitude direction, km; $\Delta \mathrm{LON}_T$ = Titan ephemeris shift, longitude direction, km.

The matrix P, which maps Titan ephemeris perturbations to corresponding changes in the target variables, is given by

$$P = \begin{bmatrix} \frac{\partial d_{OCC_T}}{\partial \mathrm{RAD}_T} & \frac{\partial d_{OCC_T}}{\partial \mathrm{LAT}_T} & \frac{\partial d_{OCC_T}}{\partial \mathrm{LON}_T} \\ \frac{\partial T_{OCC_S}}{\partial \mathrm{RAD}_T} & \frac{\partial T_{OCC_S}}{\partial \mathrm{LAT}_T} & \frac{\partial T_{OCC_S}}{\partial \mathrm{LON}_T} \\ \frac{\partial R_{C/Z}}{\partial \mathrm{RAD}_T} & \frac{\partial R_{C/Z}}{\partial \mathrm{LAT}_T} & \frac{\partial R_{C/Z}}{\partial \mathrm{LON}_T} \end{bmatrix}$$

$$= \begin{bmatrix} +0.00668 & -0.00617 & -0.00134 \\ +0.084 & -0.0718 & +0.076 \\ +0.67125 & -1.7 & +3.0 \end{bmatrix}$$

Numerical values for the elements of the P matrix were obtained by independently perturbing each of the Titan ephemeris components while holding the Titan B-space fixed and examining the resulting change in the target variables. An initial linearized estimate of the change in Titan B-space needed to nullify the effects of Titan ephemeris shift can be obtained by substituting Eq. (3) into Eq. (2). Thus

$$\begin{bmatrix} \Delta \theta_T \\ \Delta TF_T \\ \Delta B_T \end{bmatrix} = D^{-1} P \begin{bmatrix} \Delta \mathrm{RAD}_T \\ \Delta \mathrm{LAT}_T \\ \Delta \mathrm{LON}_T \end{bmatrix} \quad (4)$$

Table 4 Amount of shift in Titan B-space required to correct 95% Titan ephemeris uncertainties

	Titan position change		
	Radial 800 km	Latitude 1200 km	Longitude 1200 km
$\lvert\Delta\theta_T\rvert$, deg	0.06	0.08	0.003
$\lvert\Delta TF_T\rvert$, s	50	31	4
$\lvert\Delta \boldsymbol{B}_T\rvert$, km	32	259	600

With Eq. (4) and the 95% Titan ephemeris uncertainties, the corresponding shifts in the Titan B-space can be computed. The magnitudes of these shifts are shown in Table 4. Note that the longitude uncertainty in the Titan ephemeris is the main driver for the floating $|\boldsymbol{B}_T|$ strategy.

Finally, the method described is a linear targeting scheme. However, the actual targeting problem naturally has some nonlinearities. This makes it necessary to apply the above technique in an iterative manner. It was found numerically that the radial and latitude perturbations of the Titan ephemeris lead to retargeting which is quite linear, whereas the longitude perturbations of the Titan position lead to slightly greater degrees of nonlinearity. However, adequate covergence in examples has always been obtained with one or two iterations.

Clear Zone Probability and Targeting Window

To achieve Dione clear zone passage, the proposed strategy required two additional features. First, the navigation delivery to the clear zone must be accurate enough so that the probability of the ascending node passage in this region is acceptable despite trajectory delivery uncertainties. Second, the amount of float allowed for $|\boldsymbol{B}_T|$ must be large enough to accommodate the retargeting resulting from Titan ephemeris updates.

The nominal spacecraft path through the Dione clear zone centerline is shown in Fig. 4. To provide a measure of clear zone passage, an acceptable region was defined as extending approximately 1400 km on either side of the centerline, corresponding to trajectories which are shifted just far enough to contact the "corners" of the E-ring. Since each trajectory in this region traverses the same distance through the ring material, they were all assumed to be equally safe. Note that this assumes the E-ring has a homogeneous particle density along its length and across its width. The probability of being in this region provides a useful measure of clear zone passage.

The navigation delivery accuracy to the Dione clear zone was determined by mapping the Titan B-plane delivery covariance to the ascending node epoch by means of the clear zone partials with respect to the Titan B-plane parameters. The predicted Titan delivery covariance from orbit determination accuracy analysis was characterized by

$$\sigma_{\theta_T} = 0.91 \text{ deg}, \quad \sigma_{TF_F} = 9.5 \text{ s}, \quad \text{and } \sigma_{|B_T|} = 113 \text{ km}$$

and the partials were obtained from the third row of the targeting matrix D. This analysis yielded alσ delivery uncertainty of ± 738 km at the Dione clear zone. Since ± 1400 km is 1.9σ of delivery uncertainty, this yielded a 94% probability of passing through the acceptable region, assuming the trajectory was targeted for the Dione clear zone centerline.

The level of protection desired determined the size of the targeting window needed on the Titan B-plane. An estimate of the likely shift in $|\boldsymbol{B}_T|$ was obtained from the 95% values of Titan ephemeris uncertainty as given in Table 4. Assuming the ephemeris errors were uncorrelated with each other and with the trajectory delivery errors, the root sum square (rss) value determined the targeting size. This process yielded a required

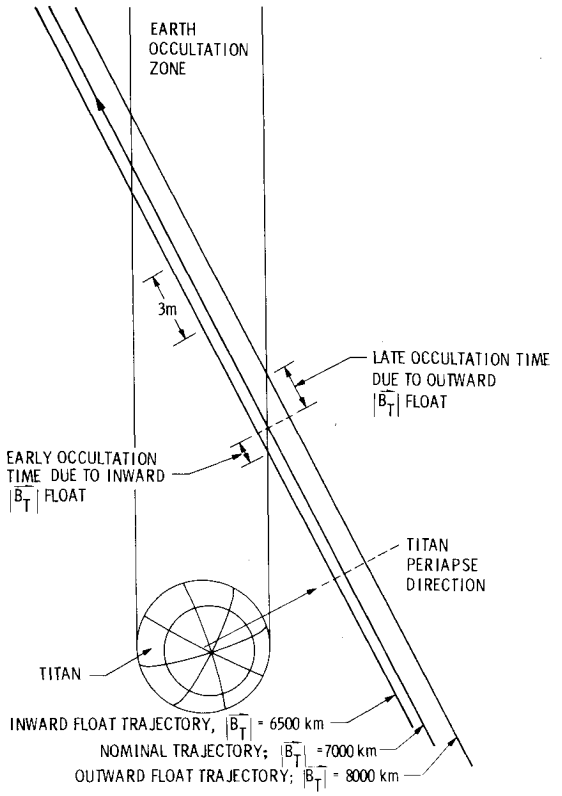

Fig. 5 Geometric effect of floating $|B_T|$ strategy on Titan science sequence event timing, trajectory plane view.

B-magnitude range of 6308-7692 km for 95% probability of being able to retarget to the clear zone centerline.

Titan Sequence

One additional implication of the targeting strategy involved the sequence of science-related events at the Titan encounter. This was a result primarily of the B-magnitude float. Figure 5 shows that an outward float causes the Titan occultations to occur at a later time. An inward float has the opposite effect.

The occultation time changes resulting from the retargeting must be accommodated in some manner. These time shifts, for 95% radial, latitude, and longitude shifts in the Titan position are 51, 63, and 66 s, respectively, which yields an rss value of ± 104 s. Since it was possible to fix only one event in time and this was chosen to be the exit time of Earth occultation by Saturn, there was nothing that could be done to eliminate the possibility of this time shift at the Titan flyby. The solution was to treat the Titan science sequence as a block which could be moved by ± 104 s.‡ The penalty, of course, was the loss of other science data acquisition for this period of time. As the spacecraft neared Saturn, optical navigation yielded the updated Titan ephemeris information. The targeting strategy was then applied and the resulting Titan sequence time offset was readily obtainable. With this information available, the block was shifted by the necessary amount.

Targeting History

The time history of the actual Voyager 1 Saturn targeting can be traced from the initial trajectory design epoch through the final TCM design epoch. This time period is divided into four segments, discussed in detail below.

‡The actual time period is somewhat longer than 104 s. This is a result of the need to shift sequence events by integral counts of the onboard timer.

1) Initial Trajectory Design Epoch (October 1979)

At this time the nominal Voyager 1 Saturn encounter trajectory was defined. As this was still about a year before the actual encounter, knowledge of the Titan ephemeris was based only on Earth-based observations. This initial trajectory was characterized by the $|B_T|$ of 7000 km, the nominal design aimpoint.

2) Final Earth-Based Update Epoch (April 1980)

By this time additional processing of Earth-based observations of Titan led to an update of that body's ephemeris. The Titan ephemeris was projected to shift (at encounter time) by +40 km in the radial direction, +100 km in the latitude direction, and +320 km in the longitude direction. According to the linear theory developed in the previous sections, this yielded a predicted shift in $|B_T|$ of −160 km. The actual $|B_T|$ shift required to null the targeting errors was −167 km, resulting in an updated $|B_T|$ of 6833 km.

3) First Approach TCM Design Epoch (Oct. 8, 1980)

The first approach TCM was performed on Oct. 10, 1980 (~Saturn − 36 days, ~Titan − 35 days). Because of the time needed to design the TCM and uplink it to the spacecraft, the orbit solution was delivered two days earlier, on Oct. 8. This solution included processing of optical navigation observations of Titan, which yielded further ephemeris shifts (at encounter time) of +169 km in the radial direction, −143 km in the latitude direction, and −26 km in the longitude direction,[17] In addition, a shift of 900 km was observed in the Saturn ephemeris. The linear theory predicted a $|B_T|$ shift of −11 km. However, the actual shift required to null the targeting errors was found to be −67 km, resulting in an updated $|B_T|$ of 6766 km. The reason for this discrepancy between predicted and actual shifts is not completely understood. The large unexpected shift in the Saturn ephemeris is a possible explanation. At this time the spacecraft was still about 44×10^6 km from the planet, about 10×10^6 km into its gravitational sphere of influence of 54×10^6 km. At this distance the spacecraft trajectory can still show significant sun-centered behavior. Thus shifts in the planet ephemeris do not imply the same shifts in the spacecraft ephemeris. This unmodeled source of targeting error could possibly account for the fact that the actual $|B_T|$ shift was different from that predicted by the linear theory, which was designed primarily to accommodate Titan ephemeris errors.

4) Final Approach TCM Design Epoch (Nov. 4, 1980)

The final approach TCM was performed on Nov. 7, 1980 (~Saturn − 6 days, ~Titan − 5 days). Again because of required TCM design and uplink time, the orbit solution was delivered three days earlier on Nov. 4. This solution included the latest optical navigation estimates of the Titan ephemeris which could be accounted for in the targeting strategy. These estimates yielded Titan ephemeris shifts (at encounter time) relative to the previous TCM epoch of +70 km in the radial direction, +117 km in the latitude direction, and −190 km in the longitude direction. The linear theory predicted a $|B_T|$ shift of +110 km. The actual shift required to null the targeting errors was found to be +94 km, yielding an updated $|B_T|$ of 6860 km. Along with this shift in $|B_T|$ there was a shift in Titan event times due primarily to the application of the targeting strategy. The shift in Titan arrival time amounted to −30 s and the shift in Titan occultation event times was −54 s, well within the allowable range of the movable Titan science sequence block.

The application of this targeting strategy for Voyager 1 at Saturn proved to be an effective means of accommodating the changing Titan ephemeris estimates and reducing the resulting targeting errors. All science and safety aim zones were achieved within acceptable tolerances. The success of science observations at Titan and Saturn has made it unnecessary for

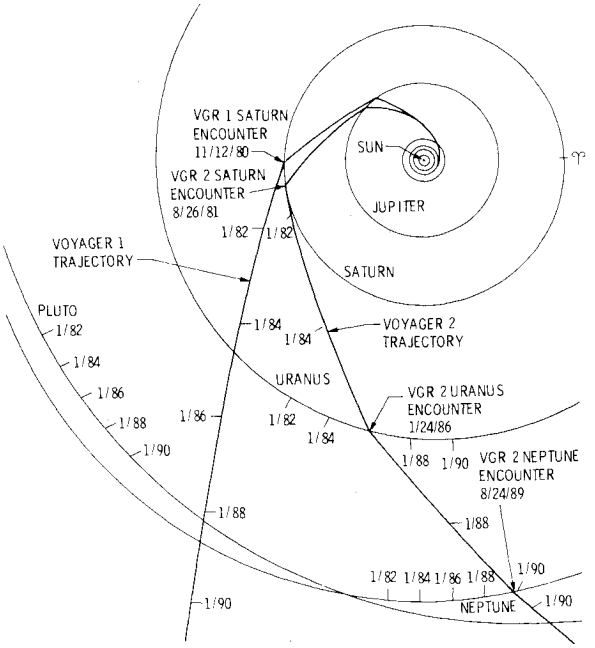

Fig. 6 Ecliptic plane projection of Voyager heliocentric trajectories.

Voyager 2 to retrace the Voyager 1 trajectory. This enabled Voyager 2 to fly to a Saturn aimpoint which will take it on to Uranus and perhaps Neptune.

Post-Saturn Trajectory

Having attained a hyperbolic orbit with respect to the sun after the Jupiter encounter, the Voyager 1 spacecraft is on a solar system escape trajectory. The Saturn encounter occurred on this departing trajectory. After Saturn, there are no further planetary encounters for Voyager 1. An ecliptic plane projection of the Voyager 1 and Voyager 2 trajectories is shown in Fig. 6. As can be seen, Voyager 1 will exit the orbits of the known planets in 1988, with Voyager 2 to follow in 1990. Also, the Voyager 1 trajectory has a high inclination (35.7 deg with respect to the ecliptic) after the Saturn encounter. The spacecraft is departing the solar system with a hyperbolic excess velocity of 16.6 km/s (3.5 a.u./year). It will reach 30 a.u. in 1987, 60 a.u. in 1995, and 100 a.u. in 2006, almost 30 years after launch. As the heliosphere boundary is expected to be somewhere between 30-60 a.u. from the sun, the spacecraft should contact this region sometime between 1987 and 1995. Voyager 1 is headed in the direction of ecliptic latitude 35.5 deg and longitude 260.6 deg. This corresponds to an Earth equatorial declination and right ascension of 12.3 and 262.2 deg, respectively, in the general direction of the constellation Ophiuchus. The closest known stellar encounter for Voyager 1 will be a 1.6 light year "flyby" of star AC + 79 3888 in about 40,000 years. This star is currently in the constellation of Ursa Minor.

Summary

This analysis has shown that, for the Voyager 1 Saturn encounter, a feasible targeting strategy was employed to reduce the negative impact on science of Titan ephemeris uncertainty. Retargeting of the trajectory to take account of late updates in Titan's position was done in a way that reduced targeting errors. Allowing the magnitude of the Titan impact vector to float within certain limits provided the necessary degree of control for reducing these dispersions. The strategy did not correct residual trajectory delivery errors. A similar approach was used for the Voyager 1 targeting at Jupiter. The method may find possible application for flyby and orbiter missions in which encounters with two or more bodies occur within a short period of time. This particular method is restricted to cases in which the relation between the target quantities and the control variables is nonsingular.

Acknowledgments

Many persons have contributed ideas, time, and effort during the course of the analysis. Special acknowledgment goes to D.L. Gray, E.L. McKinley, C.E. Kohlhase, E.D. Miner, J.P. McDanell, P.A. Penzo, L.A. D'Amario, and A.B. Sergeyevsky. Additional acknowledgment goes to D.B. Smith and R.T. Mitchell for their helpful discussions and to S. M. Gibbs and G. Peralta for their assistance in the preparation of the manuscript.

This paper presents one phase of research carried out at the Jet Propulsion Laboratory, California Institute of Technology, under Contract NAS7-100 sponsored by the National Aeronautics and Space Administration.

References

[1] Gray, D.L. and Van Allen, R.E., "Voyager Jupiter Maneuver Targeting Strategies," *Proceedings of the AIAA/AAS Guidance and Control Conference,* Danvers, Mass., Aug. 1980.

[2] "Mariner Mars 1969 Project Report, Performance," Jet Propulsion Laboratory, Pasadena, Calif., NASA TR 32-1460, Vol. II, March 1, 1971.

[3] "Mariner Venus-Mercury 1973 Project Final Report, Venus and Mercury I Encounters," Jet Propulsion Laboratory, Pasadena, Calif., NASA TM 33-734, Vol. I, Sept. 15, 1976.

[4] "Mariner Venus-Mercury 1973 Project Final Report, Extended Mission-Mercury II and III Encounters," Jet Propulsion Laboratory, Pasadena, Calif., NASA TM 33-734, Vol. II, Dec. 1, 1975.

[5] Frauenholz, R.B., "Maneuver Strategy for a Possible Pioneer 11 Extended Mission," AAS/AIAA Astrodynamics Conference, Vail, Colo., July 1973.

[6] Frauenholz, R.B. and Brady, W.F., "Maneuver Sequence Design for the Post-Jupiter Leg of the Pioneer Saturn Mission," *Journal of Spacecraft and Rockets,* Vol. 14, July 1977, pp. 395-400.

[7] Frauenholz, R.B. and Ball, J.E., "A Summary of the Pioneer 10 Maneuver Strategy," *JPL Quarterly Technical Review,* Vol. 2, Oct. 1972, pp. 46-61.

[8] Frauenholz, R.B. and Farless, D.L., "Earth-Line Maneuver Strategies for the Extended Pioneer 11 Jupiter/Saturn Mission," *Journal of Spacecraft and Rockets*, Vol. 12, May 1975, pp. 271-279.

[9] Ingersoll, A.P., Orton, G.S., Münch, G., Neugebauer, G., and Chase, S.C., "Pioneer Saturn Infrared Radiometer: Preliminary Results," *Science*, Vol. 207, Jan. 25, 1980, pp. 439-443.

[10] Penzo, P.A. and Sergeyevsky, A.B., "Voyager Mission Design for Saturn Encounter," AIAA Paper 78-1434, Aug. 1978.

[11] Feibelman, W.A., "Concerning the 'D' Ring of Saturn," *Nature*, Vol. 214, May 20, 1967, pp. 793-794.

[12] Gehrels, T. et al., "Imaging Photopolarimeter on Pioneer Saturn," *Science*, Vol. 207, Jan. 25, 1980, pp. 434-439.

[13] "New Saturn Sightings," *Sky and Telescope*, Vol. 59, April 1980, p. 296.

[14] Humes, D.H., O'Neal, R.L., Kinard, W.H., and Alvarez, J.M., "Impact of Saturn Ring Particles on Pioneer 11," *Science*, Vol. 207, Jan. 25, 1980, pp. 443-444.

[15] Dallas, S.S. and Diehl, R., Jet Propulsion Laboratory, private communication, Oct. 16, 1975.

[16] Lieske, J.H., Jet Propulsion Laboratory, private communication, April 1980.

[17] Campbell, J.K., Jet Propulsion Laboratory, private communication, March 9, 1981.